ORNL/SPR-2021/2035

High-Temperature Steam Oxidation of Irradiated FeCrAl in the Severe Accident Test Station

Nuclear Technology Research and Development

Prepared for
U.S. Department of Energy
Nuclear Technology R&D
Advanced Fuels Campaign

Authors:
Y. Yan, K. Linton, J. M. Harp, Z. Burn,
T. Jordan, B. Johnston
Oak Ridge National Laboratory

May 2021
M3FT-21OR020204074

ACKNOWLEDGMENTS

This research was sponsored by the Advanced Fuels Campaign Program of the US Department of Energy (DOE), Office of Nuclear Energy. The report was authored by UT-Battelle under Contract No. DE-AC05-00OR22725 with the US Department of Energy.

SUMMARY

FeCrAl-UO2 test capsules were fabricated at Oak Ridge National Laboratory (ORNL) and irradiated at the Advanced Test Reactor. Following irradiation, samples were sectioned from the irradiated rod and oxidation kinetics were evaluated to access the candidate cladding high-temperature oxidation performance following irradiation. The irradiation was performed at approximately 400°C to a burnup of 10 GWd/MT. The high-temperature oxidation tests were conducted in the ORNL Severe Accident Test Station at 1200 and 1300°C. Weight measurements were taken before and after oxidation testing. Cross-sections of the cladding were metallographically mounted and optical microscopy was performed. Measurements of the oxidation layer before and after high-temperature testing were collected. The results indicate the irradiated FeCrAl C35M alloy provided good thermal stability up to 1200°C.

CONTENTS

FIGURES

TABLES

ACRONYMS

AFC	Advanced Fuels Campaign
ATF	accident-tolerant fuel
ATR	Advanced Test Reactor
IFEL	Irradiated Fuels Examination Laboratory
ID	inner diameter
INL	Idaho National Laboratory
LOCA	loss-of-coolant accident
OD	outer diameter
ORNL	Oak Ridge National Laboratory
PIE	post-irradiation examination
SATS	Severe Accident Test Station

HIGH-TEMPERATURE STEAM OXIDATION OF IRRADIATED FeCrAl IN THE SEVERE ACCIDENT TEST STATION

1. INTRODUCTION

Enhanced accident-tolerant fuels (ATFs) are being developed for deployment in commercial light water reactors through a collaboration of the Department of Energy Office of Nuclear Energy (DOE-NE) Advanced Fuels Campaign (AFC) and US fuel vendors. The first fueled irradiation experiments on ATF concepts, referred to as ATF-1, began at the Idaho National Laboratory (INL) Advanced Test Reactor (ATR) in 2014. These irradiations were meant to screen many different concepts to ensure fuel–cladding compatibility and provide irradiated material for future testing. The irradiation included three FeCrAl-UO_2 drop-in rodlets fabricated at Oak Ridge National Laboratory (ORNL) targeting burn-up values of 10 GWd/MT, 30 GWd/MT, and 50 GWd/MT. The lowest burn-up capsule (ATF-18) completed irradiation and initial post-irradiation examination (PIE) at INL [1]. The capsule was shipped to ORNL's Irradiated Fuels Examination Laboratory (IFEL) hot cell facility for additional PIE in the Severe Accident Test Station (SATS). This report describes high-temperature oxidation testing of small ring specimens harvested from the irradiated rodlet. Pre- and post-testing weight measurements were taken to determine the weight gain. Cross-section images of the specimens were taken to measure the oxidation layer.

2. FeCrAl ATR IRRADIATION SUMMARY

ORNL has three loss-of-coolant-accident (LOCA) capsules for irradiation within the ATR: ATF-17, ATF-18 and ATF-19. The ATF-18 capsule contained an early variation of a FeCrAl alloy called C35MN, which is Fe-13Cr-5Al with minor additions of Mo and Nb [2]. The cladding was filled with UO_2 pellets and irradiated to a 10.4 GWd/mtU burnup [3]. The tubes used in this irradiation were created by gun drilling, not by extrusion, which is the typical method of fabricating cladding tubing. The gun drilling created a non-prototypic microstructure in the tube, but this difference is inconsequential in studying fuel-cladding interaction. The gun-drilled nature of the tube also raised suspicions that the tube itself might be vulnerable to brittle microcracking. Before the capsule was shipped to ORNL, PIE was performed [1]. The capsule was checked on GASR before being disassembled, and fission gas was detected in the capsule. The fission gas release for the fuel was found to be 0.35%, which is in line with expectations from the Vitanza curve for irradiated UO_2 fuel [4]~~[4]~~. No obvious flaws were detected in visual exams or neutron radiography. Figure 1 shows the neutron radiography results for the ORNL LOCA ATF-18 rodlet, which includes cracking in the UO_2 pellets [1]. There was some measurable change in the cladding diameter, as can be seen. The cladding diameter measures greater than the maximum reported diameter of 9392 µm in the as-built documentation, so there may be some irradiation or thermally induced cladding strain.

3. STEAM OXIDATION OF ATF-18 SPECIMENS

After irradiation and nondestructive examination at INL, the ATF-18 rodlet was shipped to the ORNL hot cells. The irradiated rodlet was sectioned into several samples for high-temperature steam oxidation tests. During sectioning, it was noted that the fuel was not firmly bonded to the cladding and could be readily removed from small cladding slices. This was expected for a drop-in style irradiation in ATR where there is no external pressure to drive the cladding creep-down that in normally seen in light water reactors. To prepare for high-temperature oxidation testing, the fuel was dissolved from segments of the cladding. High-temperature stem oxidation tests of the ATF-18 rodlet were performed in the SATS at the IFEL. SATS consists of two modules: one for integral testing of LOCA scenarios and the other with a high-temperature

furnace for testing fuel segments [5]~~[5]~~, [6]~~[6]~~. The LOCA furnace has been successfully used in LOCA fragmentation tests on high-burnup fuels [7]~~[7]~~[8]~~[8]~~[9]~~[9]~~. The tests of irradiated FeCrAl C35MN specimens in this report were conducted with the high-temperature furnace. Figure 2 shows the specimen holder used in this work.

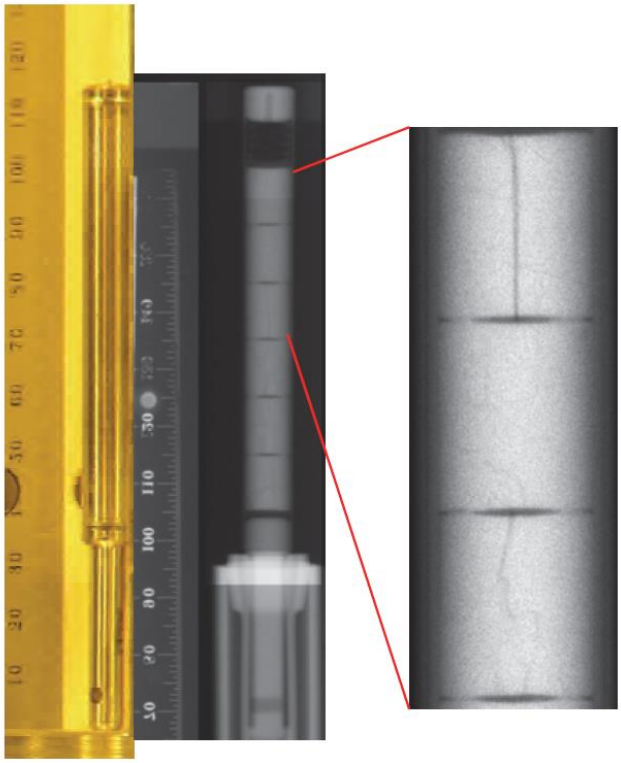

Figure 1. Visual examination and neutron radiography of the ORNL LOCA FCA-L3 rodlet with a neutron radiography detail that shows cracking in the UO2 pellets. [1]

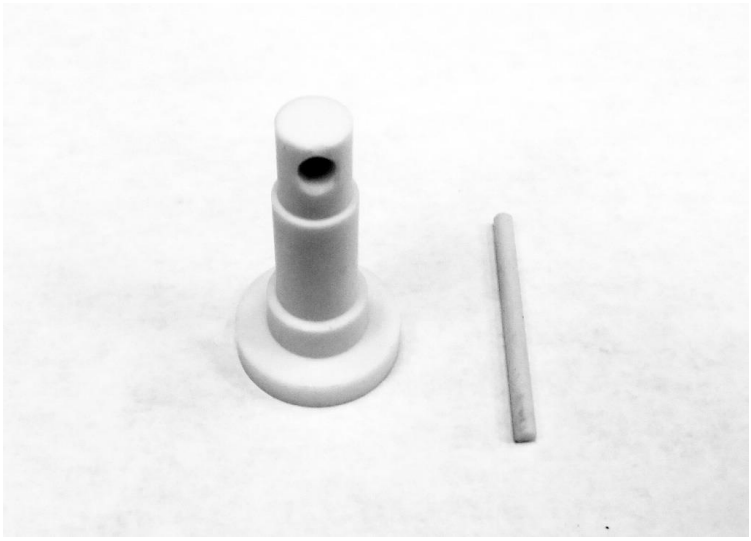

Figure 2. Specimen holder used for the SATS high-temperature steam oxidation tests.

3.1 Steam Oxidation Tests with Unirradiated ATF-18 Surrogates

Before the in-cell oxidation tests of the irradiated ATF-18 specimen, out-of-cell benchmark tests were conducted on C35MN surrogates (same alloy, heat, and fabrication procedure) to provide baseline data for the in-cell tests. These out-of-cell tests with unirradiated C35MN surrogates parallel the thermal history of the in-cell tests with irradiated AFT-18 specimens, particularly to see how the FeCrAl alloy C35MN tubing would perform at temperatures ≥1200°C. All tests were performed at atmospheric pressure with the tube in the sample holder shown in Figure 2. The surrogate specimens were approximately 9.40 mm in outer diameter (OD) and 12.50 mm long.

The specimen was first ramped from room temperature to 600°C under an argon atmosphere at a rate of 20°C/min. Following this test segment, the argon supply was shut off, steam was supplied to the test section, and the temperature was ramped to 1200°C at 7.5°C/min. The sample was held at 1200°C for one min and then slowly ramped to 1300–1400°C at 1.82°C/min to avoid temperature overshoot. Steam was supplied to the test section by injecting water into a preheat furnace at ≈0.056 g/s (200 mL/h). The tests and the temperature at which the tests were stopped are illustrated in Figure 3. Following the steam oxidation runs, the specimens were weighed.

To determine an accurate post-test specimen weight, it is important that the specimen be free of moisture. In this work, the specimens were dried in stagnant air for at least 2 hours. The drying time was verified by weight measurements: the specimen weight continued to decrease during the drying process until it reached a minimum and held at that minimum. The post-test specimen weight was measured to the nearest 0.1 mg using a calibrated balance. The weight gain was determined by subtracting the pretest weight from the post-test weight and normalizing this value to the steam-exposed surface area of the specimen. The surface area of the specimen was calculated by including the inner tube surface, the outer tube surface, and both ends.

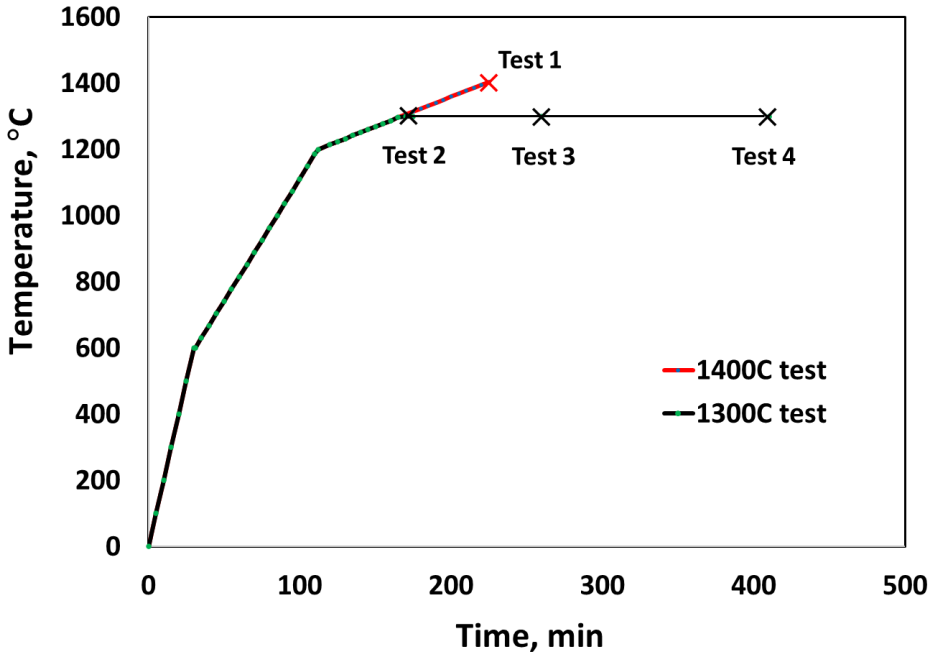

Figure 3. Heating segment illustration for out-of-cell high-temperature steam oxidation tests.

Table 1 lists the test conditions and weight gain results from the steam oxidation tests of FeCrAl alloy C35MN tubing specimens. Specimens melted as soon as the temperature reached 1400°C. However, the

C35MN was very stable at 1300°C. Post-test images of these tests are provided in Figure 4. It is generally believed that the oxidation pickup of the FeCrAl alloy is characterized by a parabolic rate law. For the oxidation tests at 1300°C, the ramp-up and cooling durations were the same. Therefore, the oxidation at the hold temperature can be considered an isothermal process. and the oxidation rate can be considered a constant for the multi-oxidation tests at a target temperature.

Figure 5 shows oxidation parabolic curves of the unirradiated C35MN specimens oxidized at 1300°C. The test data points vs. the isothermal oxidation time are in good agreement with a linear fit to the experimental data, which indicates good control of isothermal oxidation temperature. For isothermal oxidation at a target temperature of 1300°C, the weight-gain coefficient can be determined to be 3.8×10^{-9} $(mg/cm)^2/s$ by the slope of the fits in Figure 5, which is about two orders of magnitude lower than the coefficient of zirconium alloys.

Table 1. Test conditions and weight gain values for unirradiated ATF-18 surrogate C35MN tubing specimen oxidized in steam.

Test ID	Max. temperature (°C)	Time at max. temperature (min)	Measured weight gain (mg/cm^2)	Measured OD oxide μm	Measured ID oxide μm	Sample surface
1	1400	1	N/A	N/A	N/A	Melted
2	1300	1	0.336	2.1 ± 0.2	2.0 ± 0.1	Lustrous black
3	1300	90	0.586	3.7 ± 0.2	3.5 ± 0.4	Lustrous black
4	1300	240	0.762	5.4 ± 0.3	5.0 ± 0.5	Lustrous black

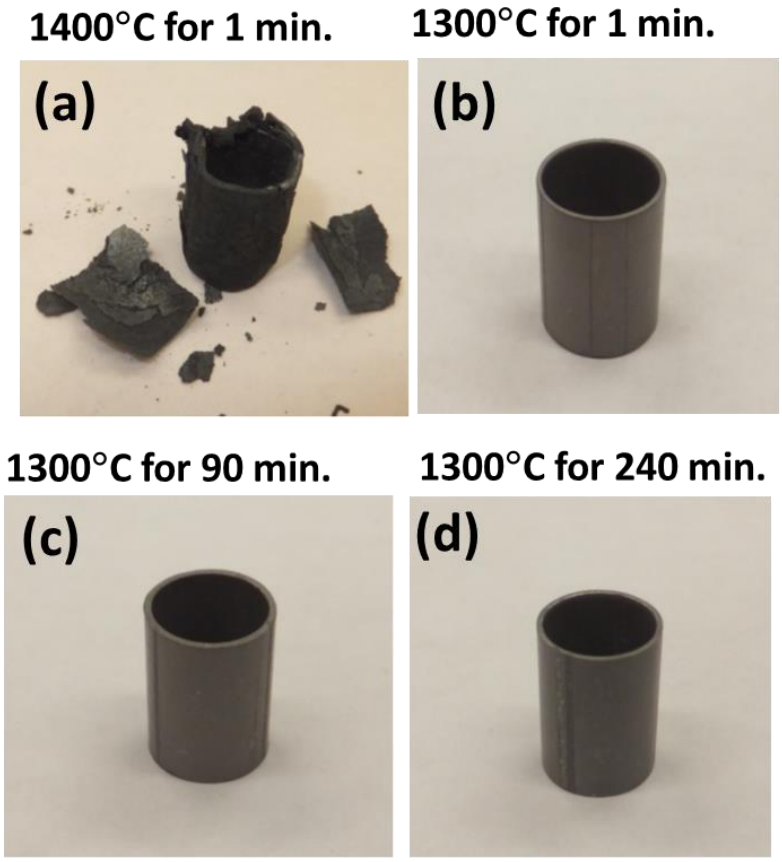

Figure 4. Post-test images of high-temperature steam-oxidized FeCrAl alloy C35MN tubing specimens.

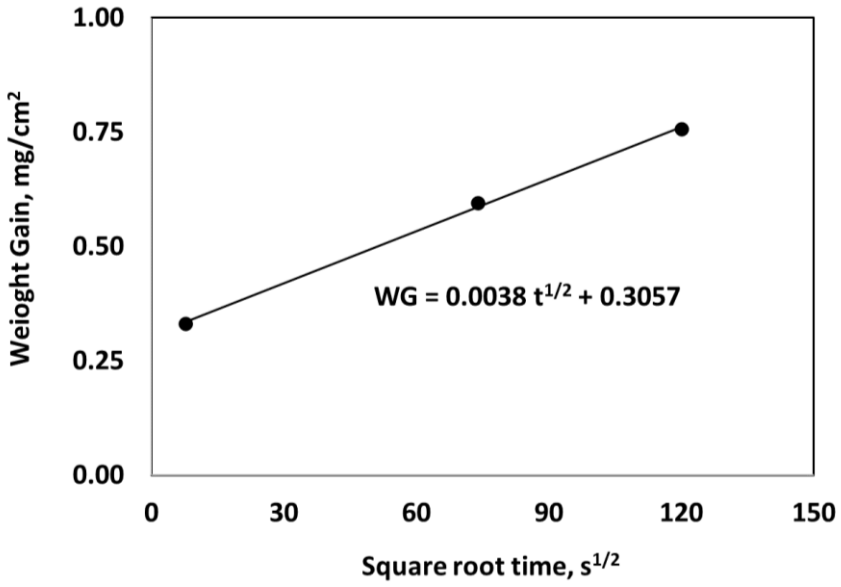

Figure 5. Steam oxidation parabolic curve of unirradiated FeCrAl C35MN at 1300°C.

The microstructure of the steam-oxidized specimens was examined. MET mounts were prepared and examined using optical microscopy to image the cross-sectional metal layers, the oxide layers, and their

interfaces. MET specimens were prepared for microstructural examination by grinding and polishing. The grinding and polishing were done with a Struers Rotoforce polisher, and a combination of SiC grit papers (500, 800, 1200, and 2400 grit paper) and then a 3 μm diamond suspension used with a polishing cloth. The polisher was set to 15 N of downward force, clockwise rotation, and a 5 minute run time. An epoxy resin was used to mount the tubing in a 1.25 in. diameter cylindrical shape to facilitate the polishing process. The images were taken digitally using a Leica microscope and were analyzed for layer thickness. No crack was observed for all specimens.

Figures 6–8 show the OD and inner diameter (ID) images for the ATF18 surrogate specimens subjected to steam oxidation at 1300°C. The thickness of the OD and ID oxide layers is quite uniform and well defined, so the oxide layer thickness was measured at four azimuthal locations (every 90°) of the cross-section of the MET mounts. The measured oxide layer thicknesses are given in Table 1.

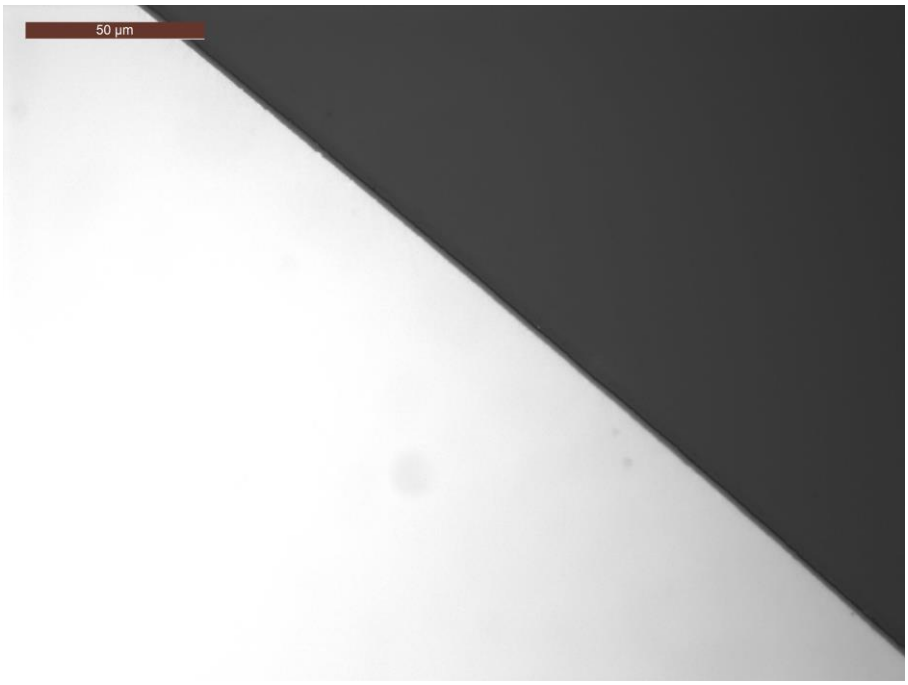

(a)

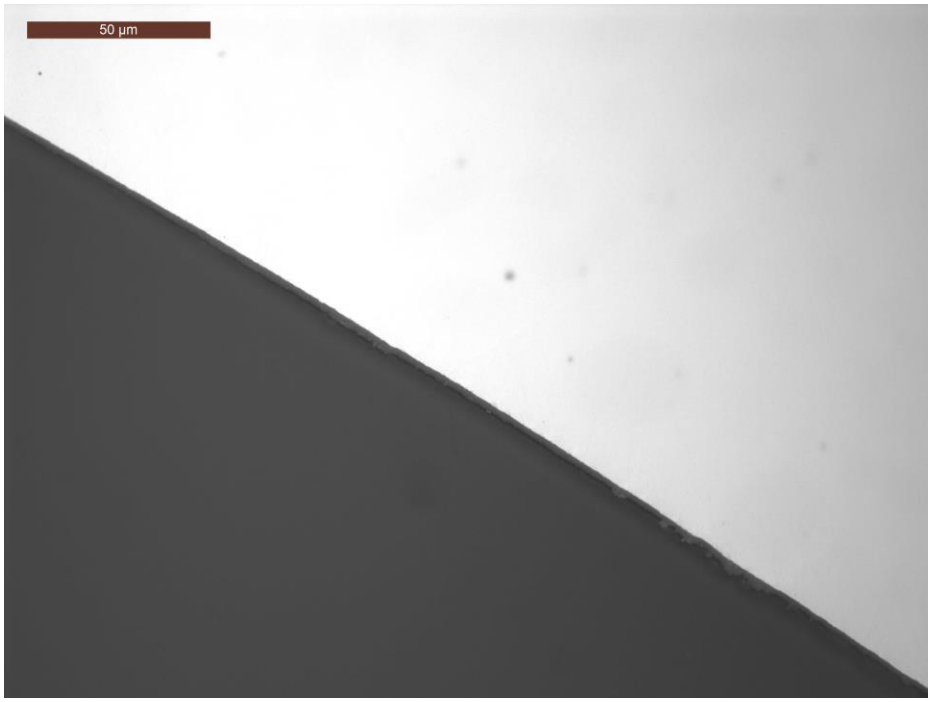

(b)

Figure 6. Micrographs of the OD (a) and ID (b) surfaces of the unirradiated C35MN oxidized in steam at 1300°C for 1 min.

(a)

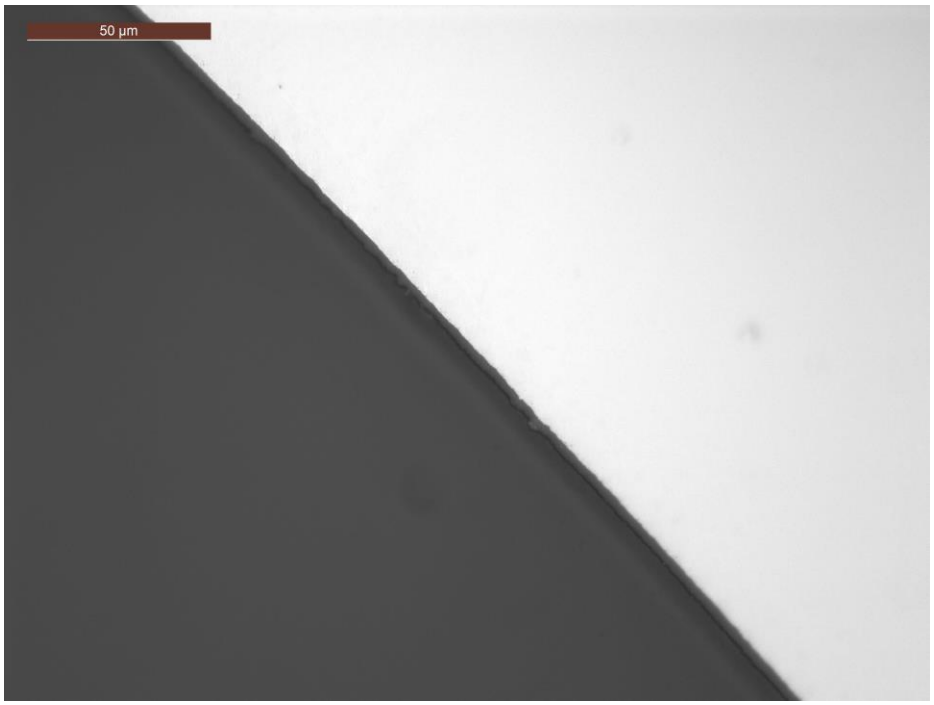

(b)

Figure 7. Micrographs of the OD (a) and ID (b) surfaces of the unirradiated C35MN oxidized in steam at 1300°C for 90 min.

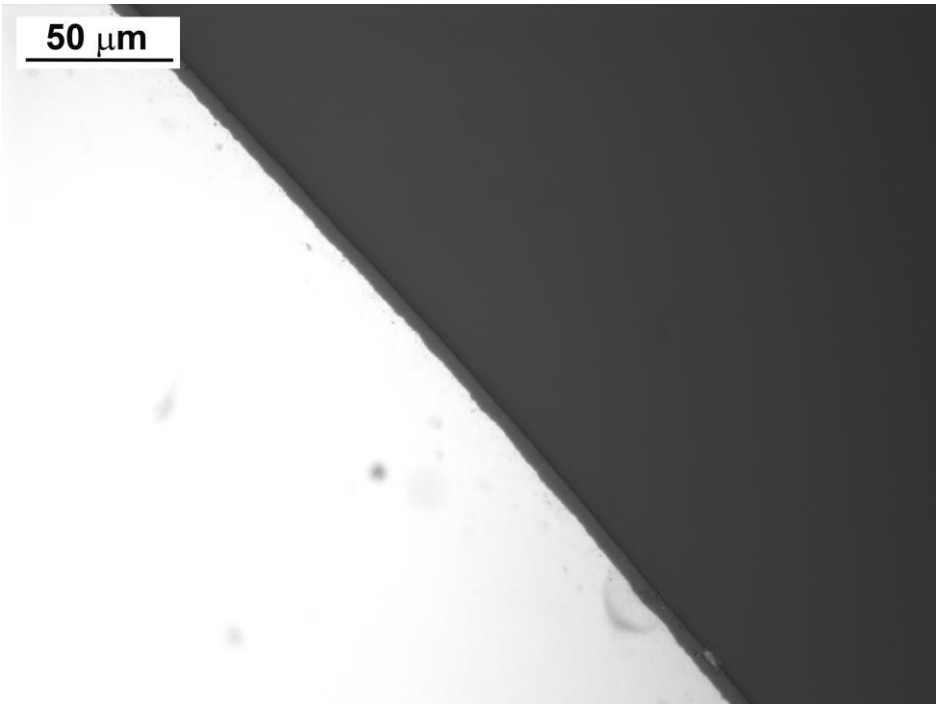

(a)

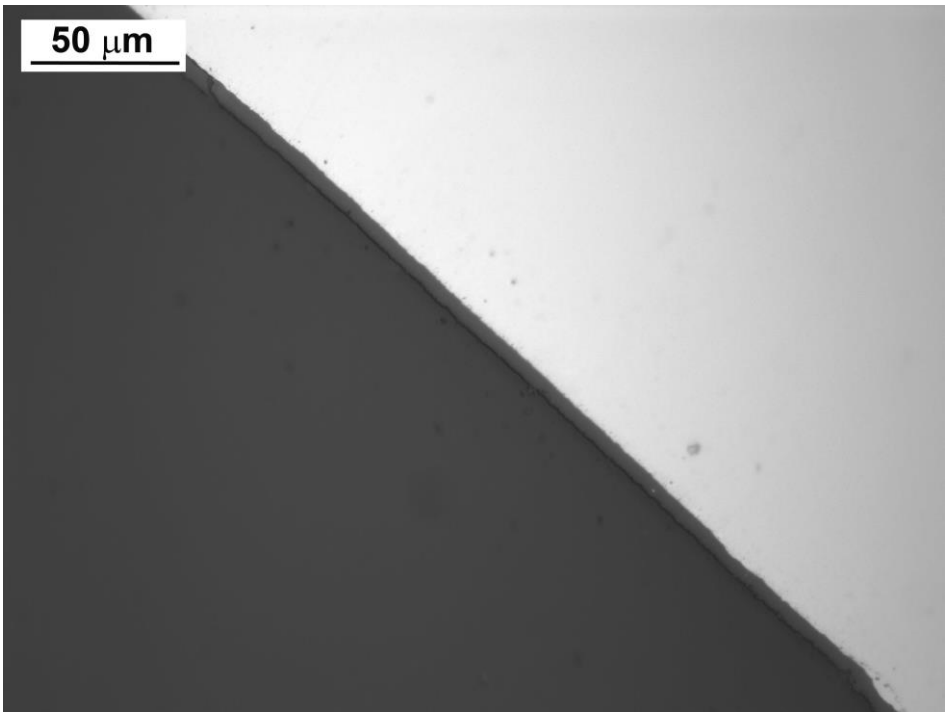

(b)

Figure 8. Micrographs of the OD (a) and ID (b) surfaces of the unirradiated C35MN oxidized in steam at 1300°C for 240 min.

3.2 Steam Oxidation Tests with Irradiated ATF-18 Specimens

Pretest characterization was performed on the ATF-18 rodlet to determine the fuel, fuel-cladding bond, and cladding behavior. Figure 9a shows a low-magnification image of the fuel morphology. The fuel partially fell out during sample preparation. The fuel-cladding bond was not found, which is not surprising for a low-burnup rod such as the ATF-18. Figure 9b is a higher-magnification image showing a gap between the cladding and fuel.

High-temperature steam oxidation tests of the irradiated ATF-18 specimens were performed with the in-cell SATS. To get a precise weight gain measurement, the fuel was dissolved in nitric acid at room temperature from segments of the cladding before high-temperature oxidation testing. The average OD of the ATF-18 rodlet was approximately 9.40 mm. The sample length for the high-temperature oxidation tests was between 4.57 and 6.96 mm.

All in-cell tests of irradiated ATF-18 specimens were conducted with the standard sample holder (see Figure 2) under the same test conditions for out-cell tests for unirradiated surrogate specimens. The specimen was first ramped from room temperature to 600°C under an argon atmosphere at a rate of 20°C/min. Following this test segment, the argon supply was shut off, steam was supplied to the test section, and the temperature was ramped to 1200°C at 7.5°C/min. The sample was either held at 1200°C or slowly ramped to 1300°C at 1.82°C/min. The tests and temperatures at which the in-cell tests were stopped are illustrated in Figure 10. Figure 11 is the temperature history of the in-cell test ATF-18G2.

Although unirradiated specimens performed very well at 1300°C, the irradiated specimens started melting as soon as the temperature reached 1300°C. However, the ATF-18 specimen was very stable at 1200°C. In addition, the oxygen pickup at 1200°C was extremely low, under the limit of the scale for weight gain measurements. Therefore, no weight gain data were reported for the ATF-18 specimens oxidized in the in-

cell SATS. Post-test images of these tests at 1200° and 1300°C are provided in Figures 12 and 13. Table 2 lists the test conditions and results of the steam oxidation tests of irradiated ATF-18 tubing specimens.

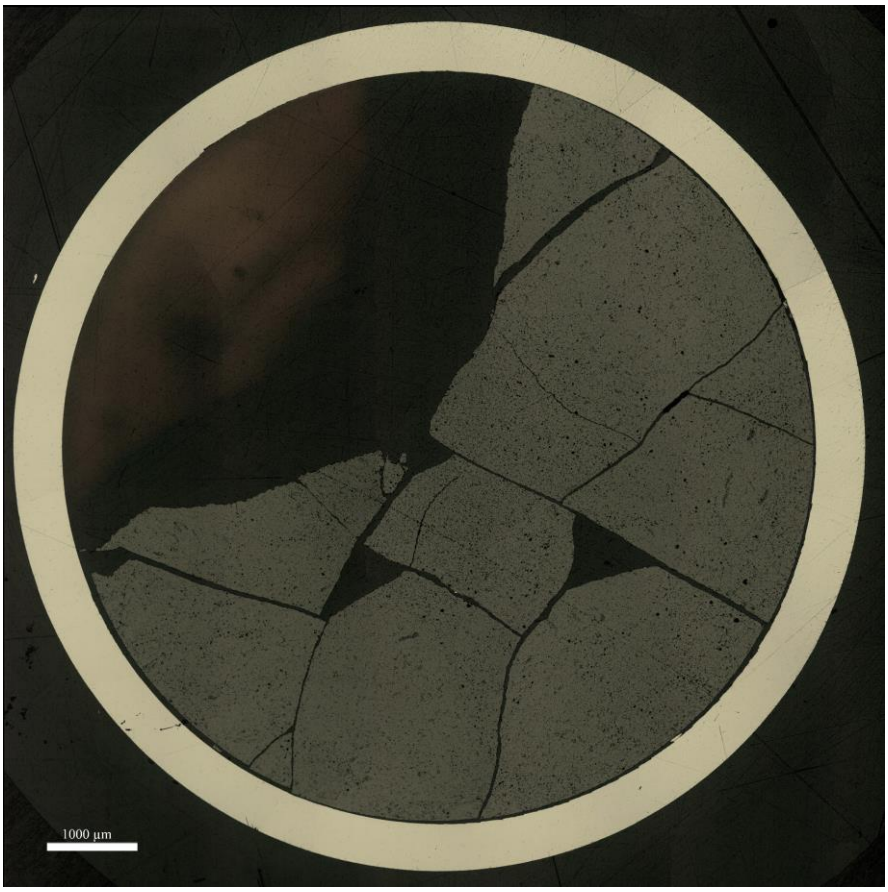

(a)

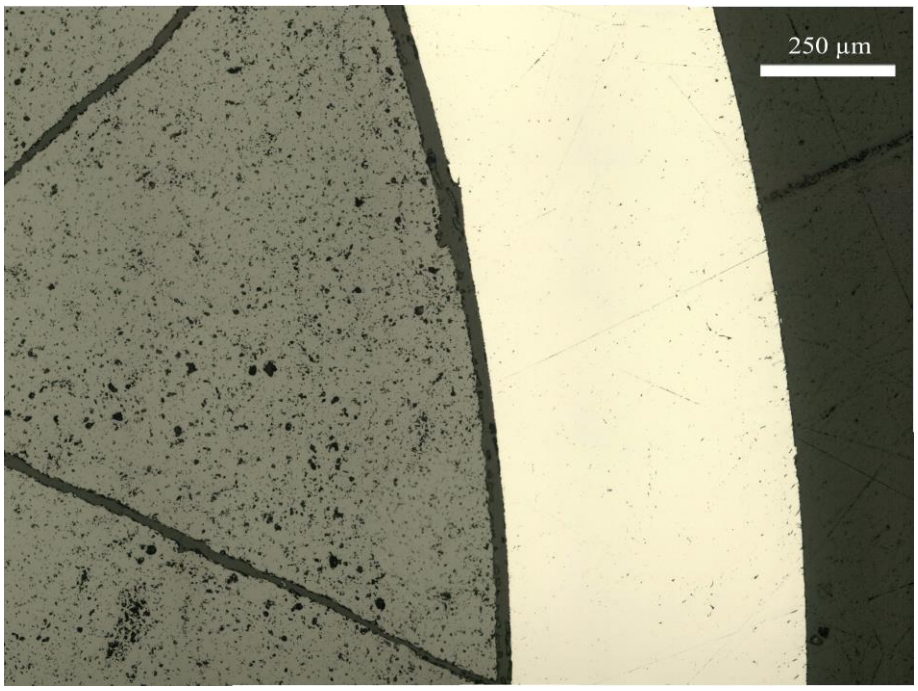

(b)

Figure 9. (a) Fuel morphology for the ATF-18 rodlet, (b) high-magnification image showing a gap between the fuel- and cladding.

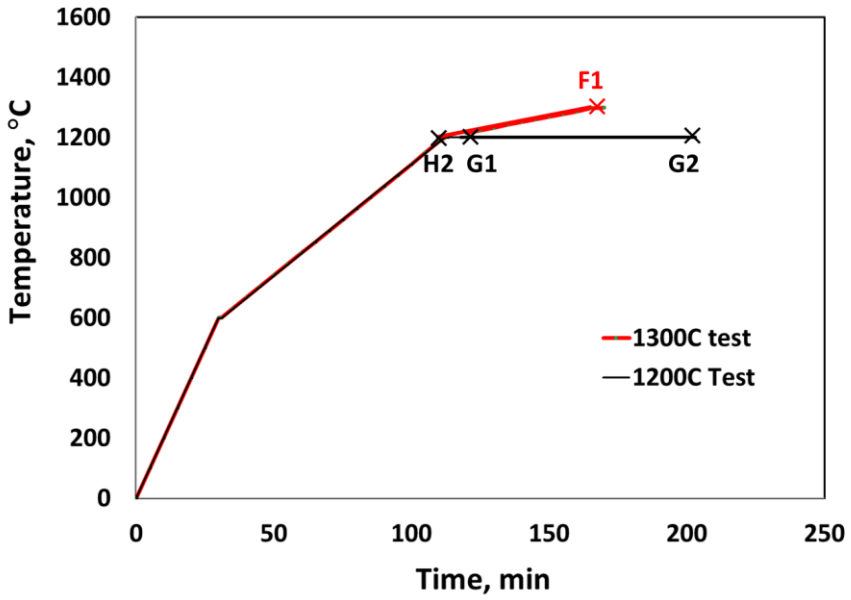

Figure 10. Heating segment illustration for in-cell high-temperature steam oxidation tests.

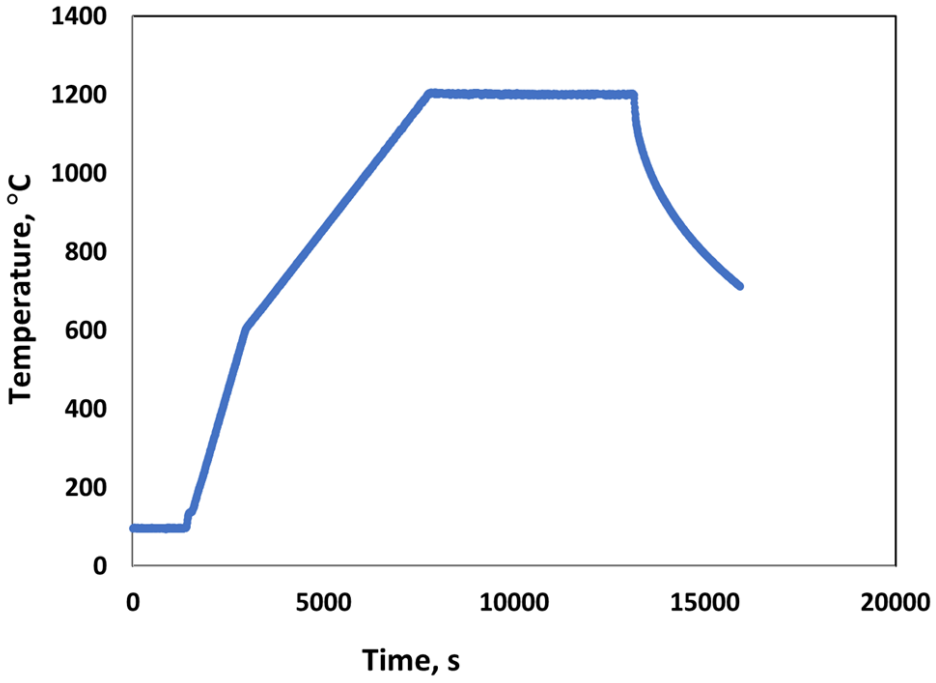

Figure 11. Temperature history of the in-cell SATS test of irradiated ATF-18G2.

Figure 12. Post-test images of irradiated ATF-18 specimens oxidized at 1200°C.

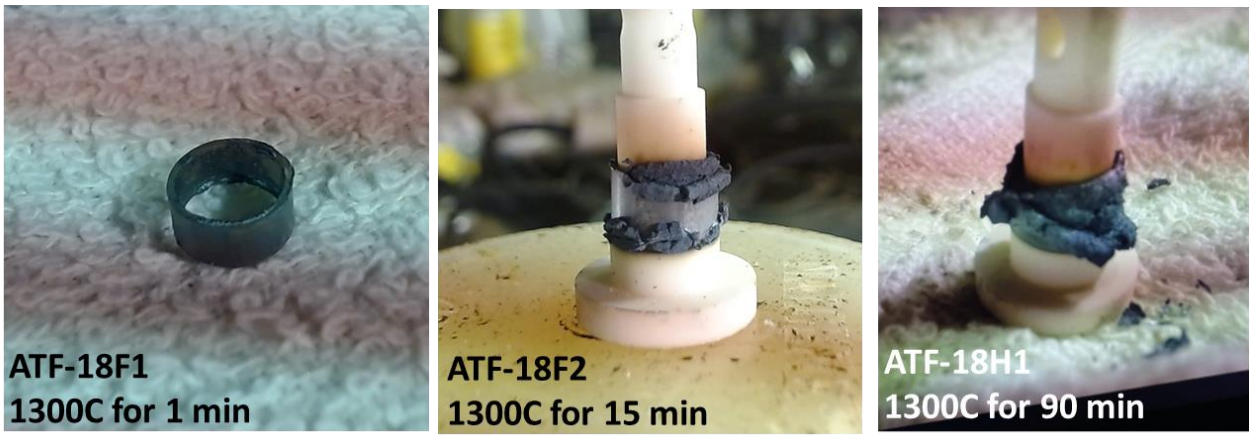

Figure 13. Post-test images of irradiated ATF-18 specimens oxidized at 1300°C.

Table 2. Test conditions and results for in-cell SATS tests of irradiated ATF-18 steam specimens.

Test ID	Max. temperature (°C)	Time at max. temperature (min)	Calculated equivalent cladding reacted for Zry-4 (%)	Sample surface
H2	1200	1	16	Lustrous black
G1	1200	15	35	Lustrous black
G2	1200	90	79	Lustrous black
F1	1300	1	–	Partially melted
F2	1300	15	–	Melted
E	1300	90	–	Melted

The microstructures of the ATF-18 oxidation specimens were examined using optical microscopy (Figures 14–21). MET specimen preparation is described in Section 3.1. The images were taken digitally using a Leica microscope. The resolution of the Leica microscope was better than 1 μ. Figure 14 shows low-magnification images for ATF-18 specimens after the high-temperature oxidation in the SATS. Micrographs at eight azimuthal locations (every 45°) of the cross-sections of the MET mounts were taken at higher magnification, as shown schematically in Figure 15.

Enhanced oxidation was observed on the inner surface at several areas of the ATF-18F1 (see Figure 14d and Figure 19), which was oxidized at 1300°C for 1 min. This phenomenon was not observed for unirradiated ATF-18 surrogate specimens oxidized in steam at 1300°C up to 240 min. For the irradiated specimens oxidized at 1200°C, the enhanced oxidation was not found. However, higher-magnification images revealed some cracks in ATF-18G1 and ATF-H2, as shown in Figures 16 and 17. The cracking appears to be initiated from the outer surface. Figure 20 is an enlarged area of the crack in Area 7 of Figure 16. The gray area on the crack surface appears to be oxide layers, which indicate the crack existed before the high-temperature oxidation test. The crack in Figure 17 is shown at high magnification in Figure 21. More study of irradiated FeCrAl alloys is needed to understand the mechanism of enhanced ID oxidation at 1300°C in Figure 19 and cracks observed in Figures 16 and 17. It is not clear when these cracks occurred. They are likely due to handling and sample preparation during PIE, but they could have occurred during irradiation or during tube fabrication. As noted in Section 2, fission gas was present in the capsule after irradiation, so it is feasible that this crack did open during irradiation, possibly as a fabrication defect.

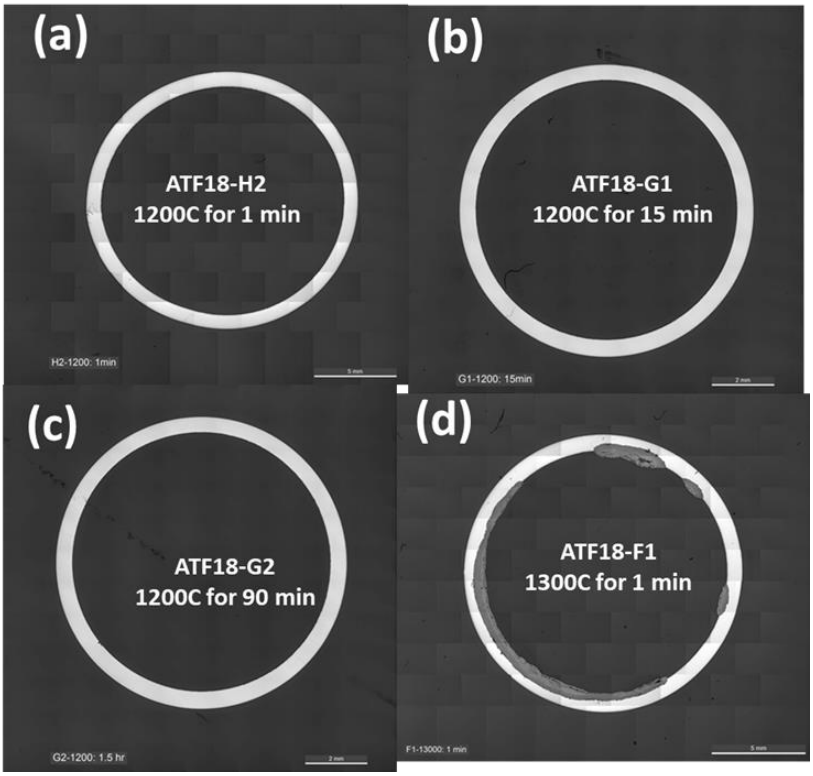

Figure 14. Low-magnification images of the irradiated ATF-18 specimens after the high-temperature oxidation in the SATS.

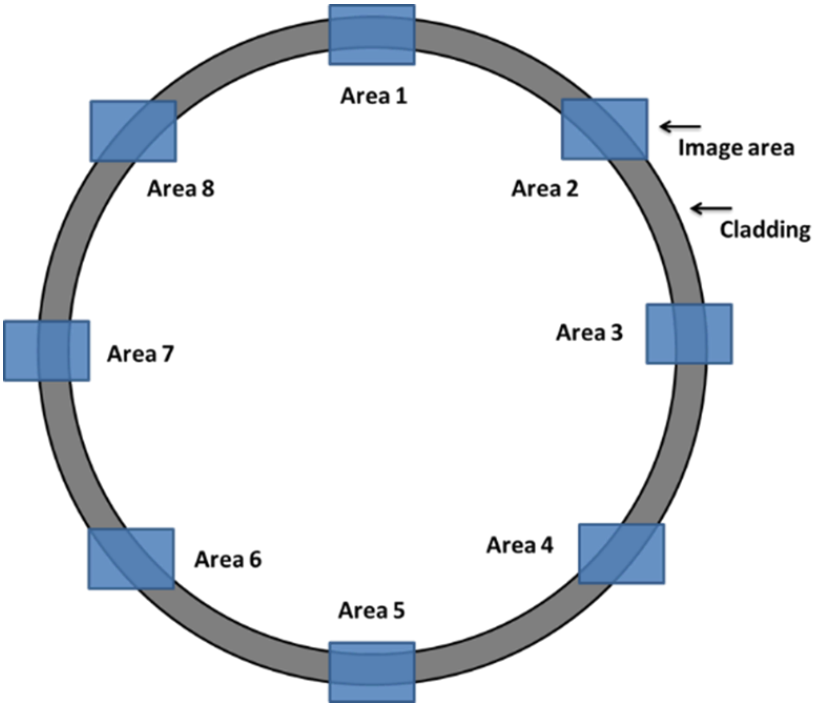

Figure 15. Schematic of eight azimuthal locations (every 45°) of the cross-section of the MET images.

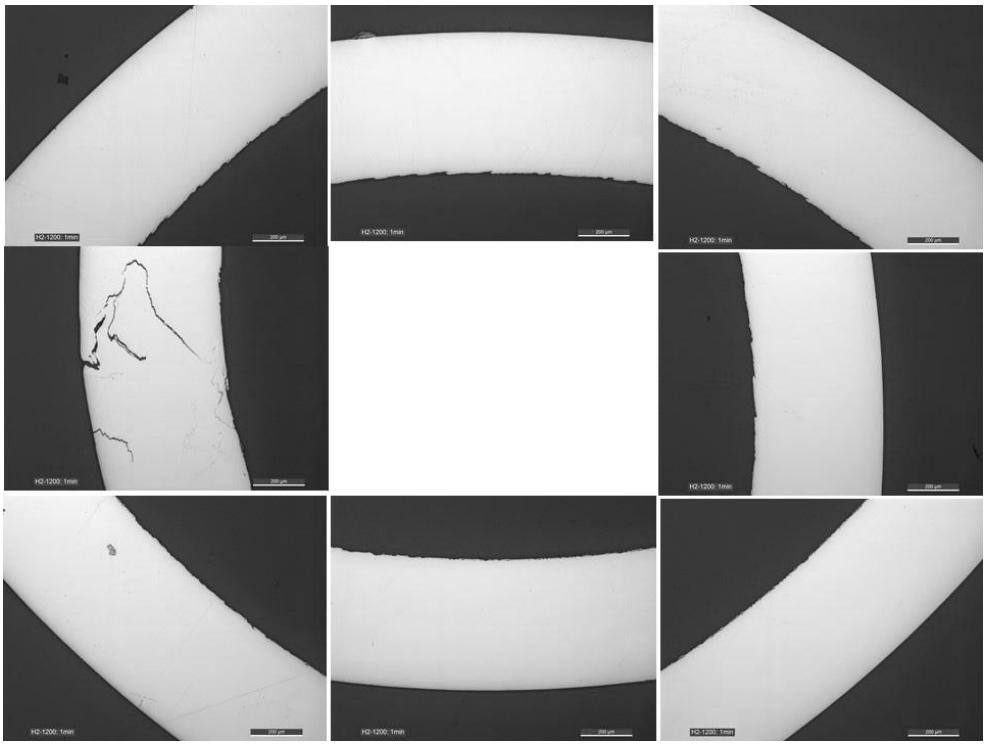

Figure 16. Images at eight locations around the circumference of ATF-18H2 specimen oxidized at 1200°C for 1 min. Cracks were observed in Area 7, initiating from the outer surface.

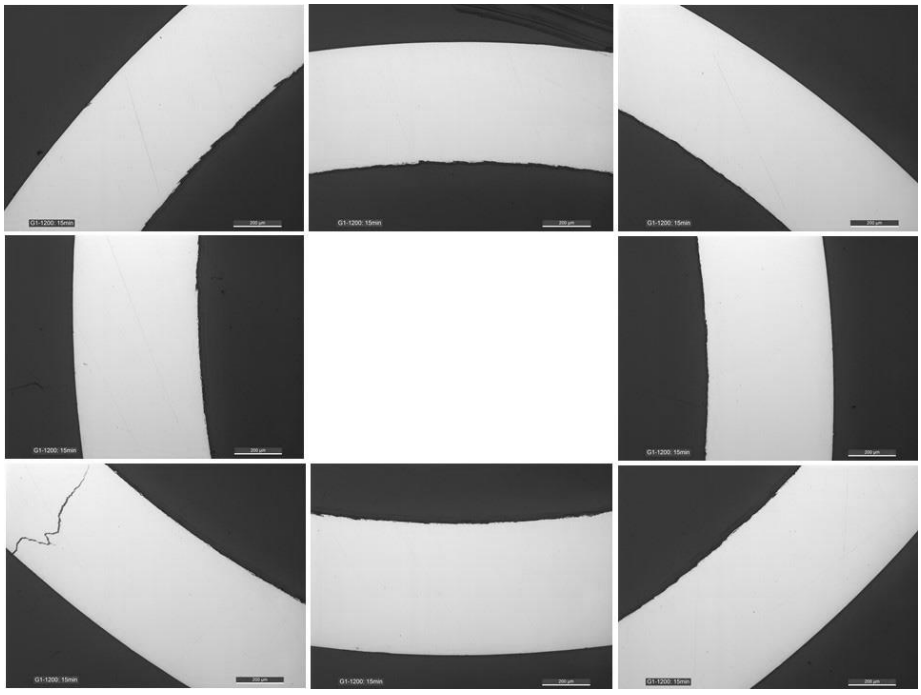

Figure 17. Images at eight locations around the circumference of ATF-18G1 specimen oxidized at 1200°C for 15 min. Cracks were observed in Area 6, initiating from the outer surface.

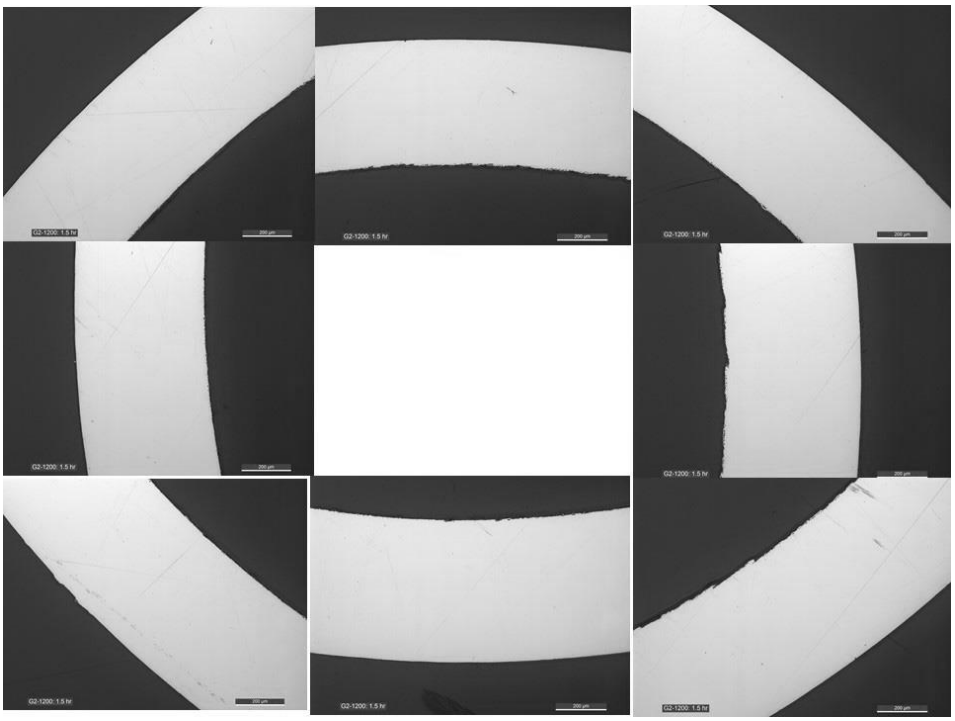

Figure 18. Images at eight locations around the circumference of ATF-18G2 specimen oxidized at 1200°C for 90 min.

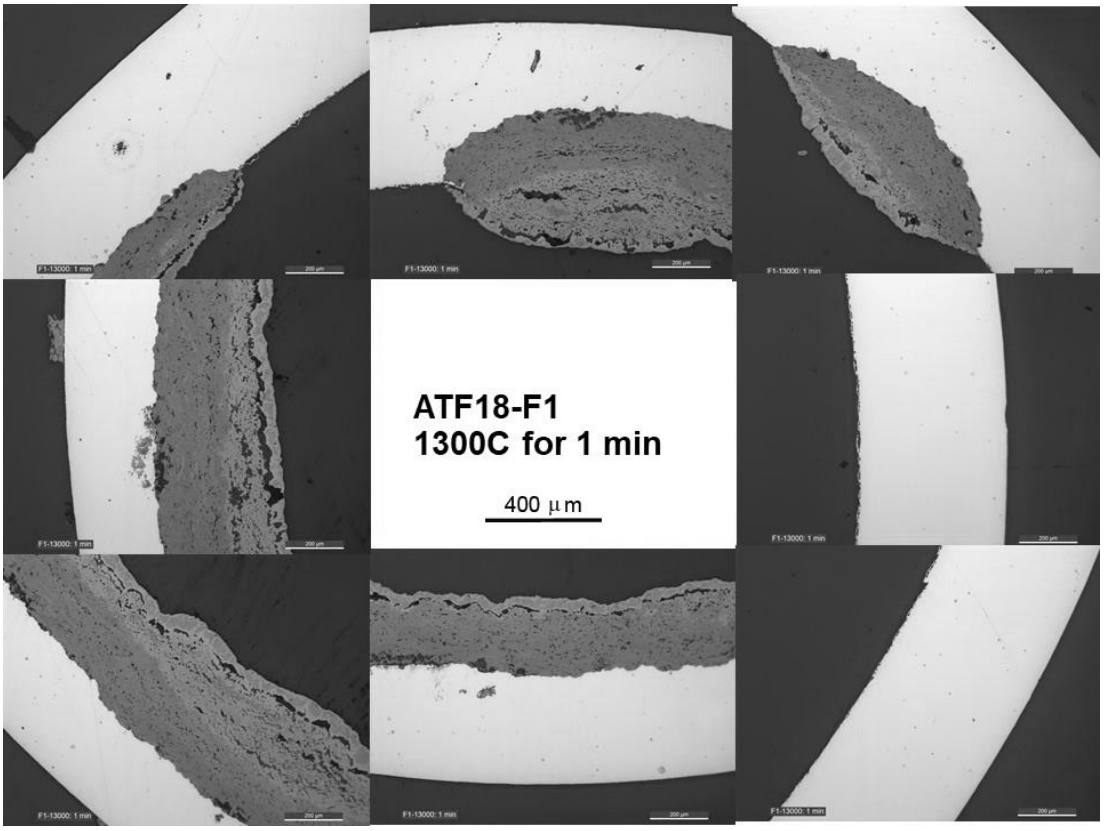

Figure 19. Images at eight locations around the circumference of ATF-18F1 specimen oxidized at 1300°C for 1 min. Local enhanced oxidation was observed on the inner surface at several areas.

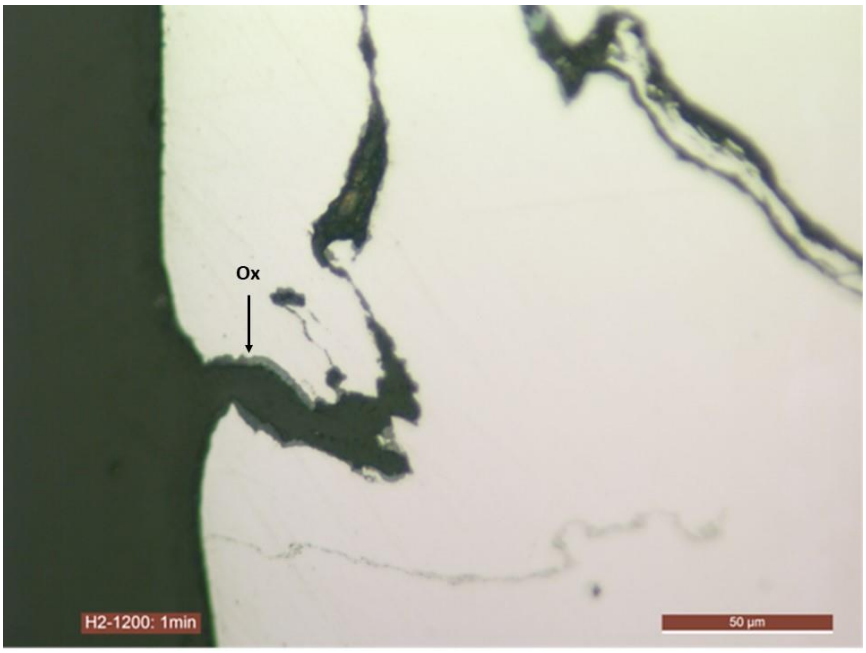

Figure 20. Higher-magnification image of the crack in Figure 16 for ATF-18H2 oxidized at 1200°C for 1 min. The gray area appears to be oxide layers formed during the high-temperature oxidation test.

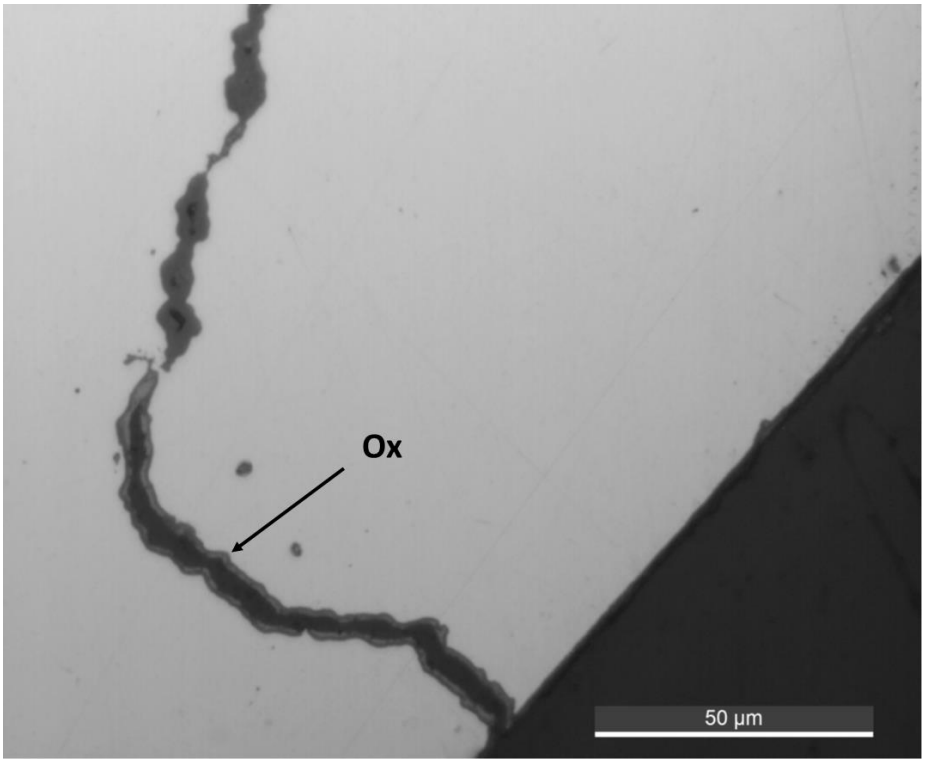

Figure 21. Higher-magnification image of the crack in Figure 17 for ATF-18G1 oxidized at 1200°C for 15 min. The gray area appears to be oxide layers formed during the high-temperature oxidation test. The specimen was rotated for higher margination images

4. CONCLUSIONS

FeCrAl-UO_2 test capsules were fabricated at ORNL and irradiated at the ATR. Following irradiation, samples were sectioned from the irradiated rod ATF-18 for oxidation kinetics study to assess the candidate cladding high-temperature oxidation performance following irradiation. The high-temperature oxidation tests were conducted in the ORNL SATS at 1200 and 1300°C. Weight measurements were taken before and after oxidation testing. Cross-sections of the cladding were metallographically mounted and optical microscopy was performed. Measurements of the oxidation layer before and after high-temperature testing were collected. The results indicate the irradiated FeCrAl C35MN alloy provided good thermal stability up to 1200°C. However, some cracks were found. The irradiated specimens started melting as soon as the temperature reached 1300°C, although the unirradiated C35MN surrogate specimens were very stable at 1300°C for 240 min. Enhanced oxidation was observed on the inner surface of the irradiated FeCrAl C35MN specimen oxidized at 1300C for 1 min. More study of irradiated FeCrAl alloys is needed to understand the mechanism of enhanced oxidation at 1300°C.

5. REFERENCES

[1] Jason M. Harp, Fabiola Cappia, and Luca Capriotti, *Postirradiation Examination of the ATF-1 Experiments—2018 Status*, INL/EXT-18-51497, September 2018.

[2] Y. Yamamoto, B. A. Pint, K. A. Terrani, K. G. Field, Y. Yang and L.L. Snead, "Development and property evaluation of nuclear grade wrought FeCrAl fuel cladding for light water reactors," *Journal of Nuclear Materials*, 467 (2015) 703-716.

[3] C. J. Murdock, B. J. Curnutt, C. Hale, *Accident Tolerant Fuels Series 1 (ATF-1) Irradiation Testing FY 2018 Status Report*, INL/EXT-18-51584, September 2018.

[4] C. Vitanza, E. Kolstad, U. Graziani, Fission gas release from UO_2 pellet fuel at high burn-up, in: *Proc. Am. Nucl. Soc. Top. Meet. Light Water React. Fuel Perform*., 1979.

[5] M. Snead, Y. Yan, M. Howell, J. Keiser, and K. Terrani, *Severe Accident Test Station Design Document*, ORNL/TM-2015/556, Oak Ridge National Laboratory, September 2015.

[6] K. Linton, Y. Yan, Z. Burns, and K. Terrani, *Hot Cell Installation and Demonstration of the Severe Accident Test Station*, ORNL/SPR-2017/434, Oak Ridge National Laboratory, August 2017.

[7] Yong Yan, Zach Burns, Tyler Smith, Kory D. Linton, Ken Yueh (EPRI), and Kurt A. Terrani, *LOCA Fragmentation Test with High Burnup HBR Fuel Rod*, ORNL/TM-2019/1239, July 2019.

[8] Yong Yan, Zachary Burns, Kory Linton, and Kurt A. Terrani, Results from In-cell Integral LOCA Testing at ORNL, WRFPM 2017, September 2017, Jeju Island, South Korea.

[9] Nathan Capps, Yong Yan, Alicia Raftery, Zachary Burns, Tyler Smith, Kurt Terrani, Ken Yueh, Michelle Bales, and ,Kory Linton, "Integral LOCA fragmentation test on high-burnup fuel," *Nuclear Engineering and Design* 367 (2020) 110811.